PROTEINS
STRUCTURE ■ FUNCTION ■ BIOINFORMATICS

Conformational fluctuations of the AXH monomer of Ataxin-1

Gianvito Grasso,[1] Marco A. Deriu,[1]* Jack A. Tuszynski,[2] Diego Gallo,[3] Umberto Morbiducci,[3] and Andrea Danani[1]

[1] Istituto Dalle Molle Di Studi Sull'intelligenza Artificiale (IDSIA), Scuola Universitaria Professionale Della Svizzera Italiana (SUPSI), Università Della Svizzera Italiana (USI), Centro Galleria 2, Manno 6928, Switzerland

[2] Department of Physics, University of Alberta, Edmonton, Alberta, Canada

[3] Department of Mechanical and Aerospace Engineering, Politecnico Di Torino, Corso Duca Degli Abruzzi 24, Torino 10128, Italy

ABSTRACT

In this paper, we report the results of molecular dynamics simulations of AXH monomer of Ataxin-1. The AXH domain plays a crucial role in Ataxin-1 aggregation, which accompanies the initiation and progression of Spinocerebellar ataxia type 1. Our simulations involving both classical and replica exchange molecular dynamics, followed by principal component analysis of the trajectories obtained, reveal substantial conformational fluctuations of the protein structure, especially in the N-terminal region. We show that these fluctuations can be generated by thermal noise since the free energy barriers between conformations are small enough for thermally stimulated transitions. In agreement with the previous experimental findings, our results can be considered as a basis for a future design of ataxin aggregation inhibitors that will require several key conformations identified in the present study as molecular targets for ligand binding.

Proteins 2016; 84:52–59.
© 2015 Wiley Periodicals, Inc.

Key words: neurodegenerative; molecular dynamics; Ataxin; replica exchange; molecular modeling; principal component analysis; clustering; free energy.

INTRODUCTION

Spinocerebellar ataxia type 1 (SCA1) is an inherited neurodegenerative disease belonging to the class of polyglutamine (polyQ) diseases. In fact, it is well established that SCA1 is mainly caused by polyQ expansion in Ataxin-1 (ATXN1), a nuclear protein constituted by 820 residues.[1] However, parallel to the well-established correlation between polyQ expansion and disease onset and severity,[2] other findings have demonstrated the importance of the AXH domain of ATXN1 in both modulating the development of the disease and influencing the aggregation process.[3–6] The structure of the AXH domain, the only globular region so far identified in ATXN1, is an asymmetric homodimer,[1] whose interface is characterized by 20-residue motifs, which mutually adapt, but are different.[7]

Recent findings have shown that ATXN1 aggregation is strongly reduced by replacement of AXH domain with the homologous sequence of the transcription factor HBP1,[5] confirming the important role of AXH in modulating the aggregation mechanism. Moreover, it was reported that the isolated AXH has the tendency to misfold and aggregate into fibers without any destabilizing factor, such as temperature increase or chemical denaturants.[5]

AXH plays a key role in physiological functions of ATXN1. It is involved in most of the known interactions that ATXN1 forms with other proteins, suggesting that it could fold as an independent domain and forms a novel protein–protein and RNA recognition motif.[8]

The fact that AXH is an unusual chameleon protein representing the first known example of the existence of alternative conformations,[9] has made the AXH domain the object of several experimental studies aimed at

Additional Supporting Information may be found in the online version of this article.

Gianvito Grasso and Marco A. Deriu contributed equally to this work.

*Correspondence to: Marco Agostino Deriu; Istituto Dalle Molle di studi sull'Intelligenza Artificiale (IDSIA), Scuola universitaria professionale della Svizzera italiana (SUPSI), Università della Svizzera italiana (USI), Centro Galleria 2, Manno 6928, Switzerland. E-mail: marco.deriu@idsia.ch

Received 21 July 2015; Revised 7 October 2015; Accepted 19 October 2015
Published online 2 November 2015 in Wiley Online Library (wileyonlinelibrary.com). DOI: 10.1002/prot.24954

© 2015 WILEY PERIODICALS, INC.

characterizing its behavior in solution under different conditions.[1,7,8,10–12]

The emerging picture is that the AXH domain shows different structural properties leading to asymmetric dimeric interfaces.[9] More in depth, despite the well-preserved tertiary and quaternary structure, the AXH domain is characterized by local structural plasticity at the N-terminal regions of each monomer, which is involved in the dimer interface.[9] Moreover, it was reported that the dimer appears to be the predominant AXH species in solution,[10] unlike the homologous sequence HBP1, which is a monomer.[8] While the existence of the AXH monomeric species has already been demonstrated, the conformational stability of the AXH monomer (hereinafter called AXH^m) in solution is a debated issue.[9] Previous works have also highlighted that the monomer is unstable in water with a tendency to aggregate.[9] Recently, it was demonstrated that the extraordinary structural plasticity of the AXH^m plays an essential role in determining the equilibrium between the physiological and pathological interactions of ATX1.[13] Despite the large number of experimental studies focused on the AXH domain, a similar effort has not been put on the side of molecular modelling to investigate structural and dynamics of ATH^m till now. However, molecular modeling, and in particular molecular dynamics has been widely demonstrated to provide important or even exceptional insights to better understand molecular mechanisms at the basis of subcellular phenomena,[14–21] such as the ones that drive protein aggregation and protein misfolding in neurodegenerative diseases.[20,22]

This article reports on the first molecular dynamics investigation of AXH monomer conformational properties and dynamics. We made use of both biased and unbiased MD techniques. Whereas classical MD simulation have revealed the extensive conformational fluctuation of the N-terminal tail of the AXH monomer in solution, replica exchange molecular dynamics (REMD) provided a better sampling of the AXH^m state space and, the estimation of the free energy landscape characterizing the AXH^m conformational changes. In the present study, we have paid particular attention to the dimensionality reduction of the MD trajectories, applying the widely used principal component analysis (PCA) to elucidate the large-scale molecular phenomena characterizing the AXH^m folding pathway. Surprisingly with respect to previous hypothesis, our results depict the AXH monomer as a relatively stable structure with, in general, highly conserved domains except for the N-terminal tail switching among several arrangements.

MATERIALS AND METHODS

Classical molecular dynamics

The AXH monomer model coordinates ware extracted from the recently refined structure of the AXH domain[9] (for consistency with previous literature,[9] residue numbering refers to the UniProtKB/Swiss-Prot entry No. P54253 + 1). The system was fully solvated in explicitly modeled water[23] where the minimum distance between the protein and the edge of the box was 1.2 nm. The net charge of the system was neutralized by the addition of Cl− and Na+ ions. The above mentioned system (20,000 interacting particles) was first minimized by the steepest descent energy minimization algorithm followed by two preliminary position restraint MD simulations of 100 and 50 ps in NPT and NVT ensemble, respectively. The production run was performed for 1 μs in the NVT ensemble. GROMACS 4.6 package has been used for all MD simulations and data analysis.[24] AMBER99-ILDN force field[25,26] was used to define the protein topology, since its ability to provide an accurate description of protein conformational ensembles was widely demonstrated.[25,27] The TIP3P model[28] was used for representing water molecules. Electrostatic interactions were calculated at every step with the particle-mesh Ewald method with a short-range electrostatic interaction cutoff of 1.2 nm. A cutoff of 1.2 nm was also applied to Lennard–Jones interactions. The LINCS algorithm[29] approach has allowed an integration time step of 2 fs. The GROMACS *v-rescale* thermostat[30] was used to keep simulation temperature constant at 310 K. The visual molecular dynamics (VMD)[31] package was used for the visual inspection of the simulated systems. Dedicated GROMACS tools were used for a quantitative analysis in terms of root-mean-square deviation (RMSD) and root-mean-square fluctuation (RMSF). Analysis of secondary structure (SS) dynamics was performed by applying the STRIDE software.[32,33] Ramachandran plots, produced using PROCHECK,[34] were used for better insight into the atomistic changes of the AXH residues.

Replica exchange molecular dynamics and cluster analysis

REMD[35] was applied to explore the conformational ensembles of the AXH domain. In particular, 64 replicas were simulated for temperatures ranging from 310 to 480 K. Temperatures were distributed across the replicas in a geometric progression, i.e., with the same ratio used to scale each temperature from the one below it, keeping the overlap of the potential energy distributions constant across the temperature space (Supporting Information Fig. S1). The resulting exchange probability was 0.4. The exchange of replicas was attempted every 1 ps. This time interval was chosen to be large enough compared to the coupling time of the heat bath ($\tau = 0.1$ ps). Each replica was simulated for 50 ns, obtaining a cumulative simulation time of 3.2 μs. To obtain the canonical average of each physical quantity at a specific temperature, the computational data were analyzed as time average over all trajectory steps corresponding to the chosen

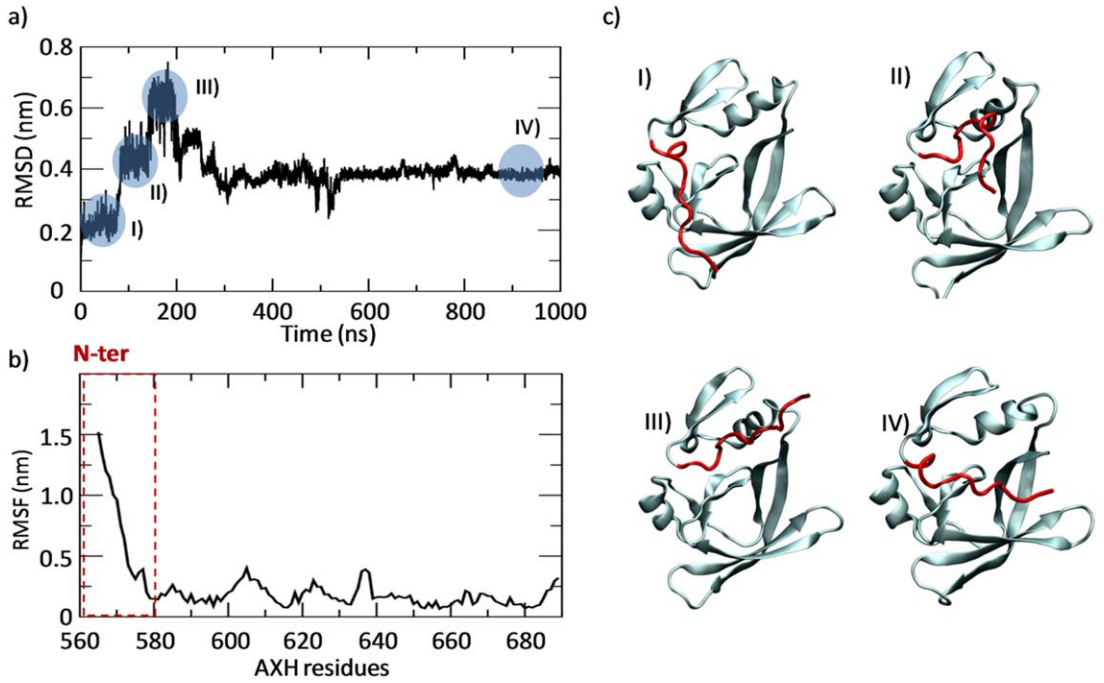

Figure 1

(**a**) C-alpha/C-alpha root mean square deviation (RMSD) calculated over the classical MD trajectory. The stability regions of the RMSD plot are highlighted by circles. For each stability point (I, II, III, and IV), the corresponding AXH monomer conformation is represented on panel c. (**b**) Root mean square fluctuation (RMSF) calculated over the classical MD trajectory of the AXH monomer in water. [Color figure can be viewed in the online issue, which is available at wileyonlinelibrary.com.]

temperature, as usually done in REMD.[36] Structure based clustering approach has been carried out to get insight into likeliness of AXH N-ter arrangements. GROMOS approach,[37] implemented in GROMACS package, was applied to the replica exchange molecular dynamics trajectory at 310 K.

Principal component analysis and free energy reconstruction

Principal component analysis (PCA) was applied to reduce the dimensionality of the system, elucidating large-scale and low-frequency modes, respectively, thus yielding collective motions directly related to a specific molecular event.[38] After the alignment of the AXH^m C-alpha Cartesian coordinates, the covariance matrix was calculated and diagonalized. To estimate the free energy landscape of the AXH^m, the first two eigenvectors derived from the PCA were used as reaction coordinates. The corresponding free energy surface along the 2-dimensional space $V = (pca1,pca2)$ is given by:

$$\Delta G(V) = -K_b T \times [\ln P(V) - \ln(P_{max})] \qquad (1)$$

where $P(V)$ is the probability distribution obtained from the histogram of the computational data taken from the MD trajectory. P_{max}, representing the maximum of the distribution, was used to ensure that $\Delta G = 0$ for the lowest free-energy minimum.

RESULTS

Classical MD

A MD simulation of 1 μs was performed to analyze the AXH^m structural properties in solution. The C-alpha-C-alpha RMSD reported in Figure 1(a), shows that the AXH^m undergoes several conformational transitions until the stability is reached (from 600 to 1000 ns). Analyzing the RMSF of the AXH^m residues [Fig. 1(b)], it is possible to identify the N-terminal domain (residues Ala565-Ile580) as mainly responsible for the protein conformational fluctuations mentioned above (RMSF= 1.5 nm). The visual inspection of the AXH^m conformational states corresponding to the stability region of the RMSD plot [reported in Fig. 1(a)] are shown in Figure 1(c), confirming the leading role of the N-terminal domain as responsible for the conformational fluctuation of the AXH^m. In greater detail, once the RMSD stability is reached (from 600 to 1000 ns), the N-terminal tail (Ala565-Pro568) is packed against Gly680-Leu688 and Asp608-Glu620 [Fig. 1(c), IV]. Figure 2 shows the AXH^m secondary structure probability, calculated by averaging the 4 monomer configurations taken from

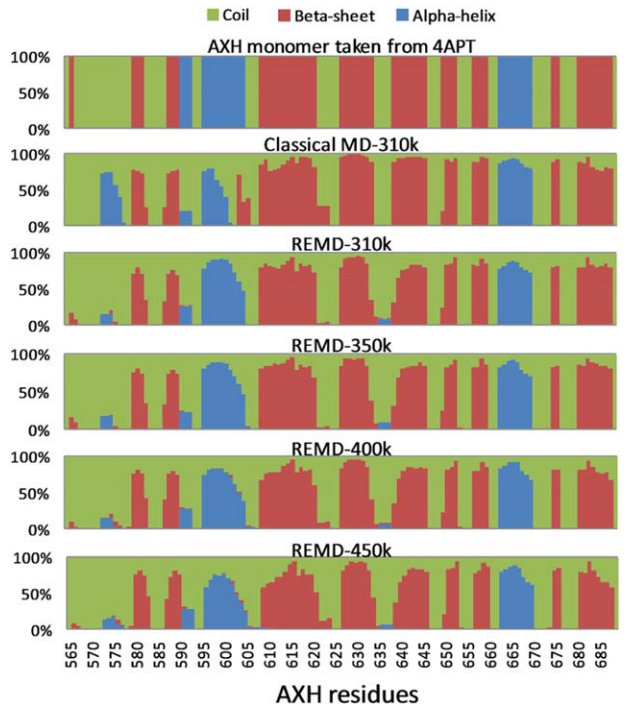

Figure 2

Secondary structure probability calculated over the monomer conformation taken from APT (as average), the classical MD simulations at the equilibrium, and REMD ensemble at different temperature.

4APT[9] and 400 configurations taken every 1000 ps from the MD equilibrium trajectories (from 600 to 1000 ns). The protein secondary structure resulted to be highly conserved, with the exception of α2 and partially α3, both characterized by an intrinsic tendency of helix-coil transition in water environment. [mt]99% of the protein residues were found in the most-favoured and additional-allowed regions of the Ramachandran plots (Supporting Information Fig. S2), providing support for the model's correctness.

Replica exchange molecular dynamics

From the REMD simulations, (i) all the temperatures were explored numerous times by each replica and (ii) acceptance ratios of more than 0.4 were obtained. The computational data were analyzed as time averages over all trajectory steps corresponding to a specific temperature, as is usually done in REMD,[36] to study the conformational variation of the AXH^m at that temperature. Interestingly, it was observed that the AXH^m secondary structure is highly conserved in the temperature range from 310 to 450 K, with the exception of α2 and (partially) α3, confirming data coming from the classical MD trajectory.

The application of the principal component analysis (PCA) allowed to highlight the large-scale and low-frequency modes mainly related to a specific protein conformational change. After the alignment of the AXH^m C-alpha atoms, the MD trajectory at 310 K was filtered to show only the motion along the first and second eigenvector, calculated by the covariance matrix diagonalization. The AXH^m RMSF calculated over the filtered trajectory (Figs. 3 and 4) clearly shows that, as expected, the first and second PCA eigenvectors are able to effectively describe the conformational changes of the N-terminal region ($RMSF_{PCA1} = 0.9$ nm and $RMSF_{PCA2} = 0.5$ nm). The free-energy landscape of AXH^m was calculated by applying [Eq. (1)] to the probability distribution of the projections along PCA1 and PCA2 taken from the REMD trajectory at 310 K. Thus, the free energy landscape shown in Figure 5 is reported in a 2-dimensional space $E = (pca1, pca2)$, where several free energy wells can be identified.

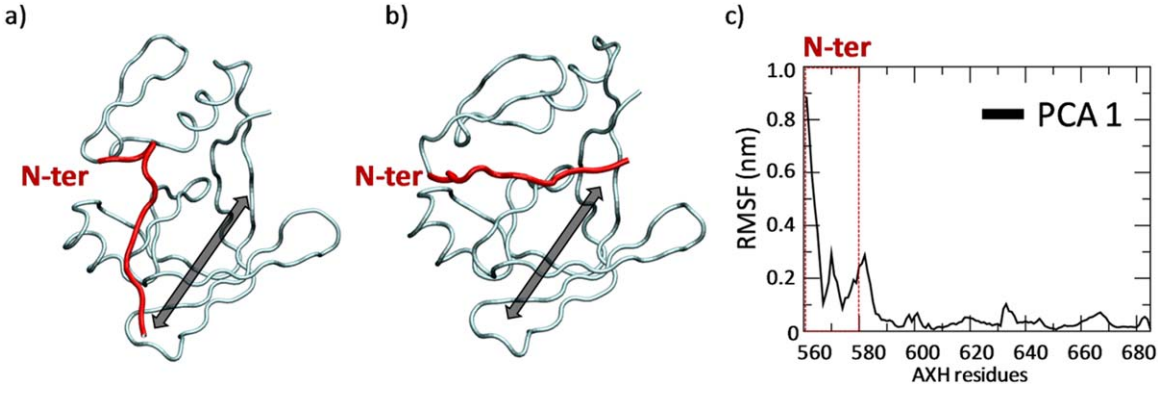

Figure 3

(**a**) and (**b**) Visual inspection of the extreme extensions along the first principal component eigenvector; (**c**) root mean square fluctuation calculated over the classical MD trajectory filtered on the first principal component eigenvector. [Color figure can be viewed in the online issue, which is available at wileyonlinelibrary.com.]

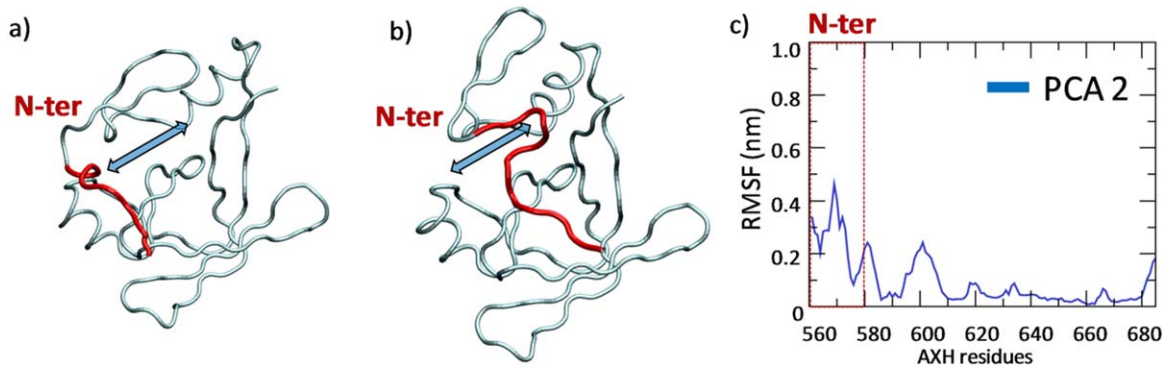

Figure 4

(**a**) and (**b**) Visual inspection of the extreme extensions along the second principal component eigenvector. (**c**) Root mean square fluctuation calculated over the classical MD trajectory filtered on the second principal component eigenvector. [Color figure can be viewed in the online issue, which is available at wileyonlinelibrary.com.]

A structure based clustering approach to get insight into other possible AXH^m conformational states, was applied to the REMD trajectory at 310 K (Fig. 6). The most populated clusters are represented in Figure 6, whereas clusters characterized by a percentage population lower than 2% over the whole trajectory steps have not been considered. Clusters A,B, C, and D are the most populated and refer to 4 N-ter different arrangements.

Moreover, cluster centroids have been also represented (in terms of first and second principal component projection values) on the free-energy landscape in Figure 5. It is worth noticing how, cluster centroids are positioned on energy wells covering mostly the whole free-energy landscape. As expected, centroids representing the most populated clusters (A,B, C, and D) fall in deepest energy minima.

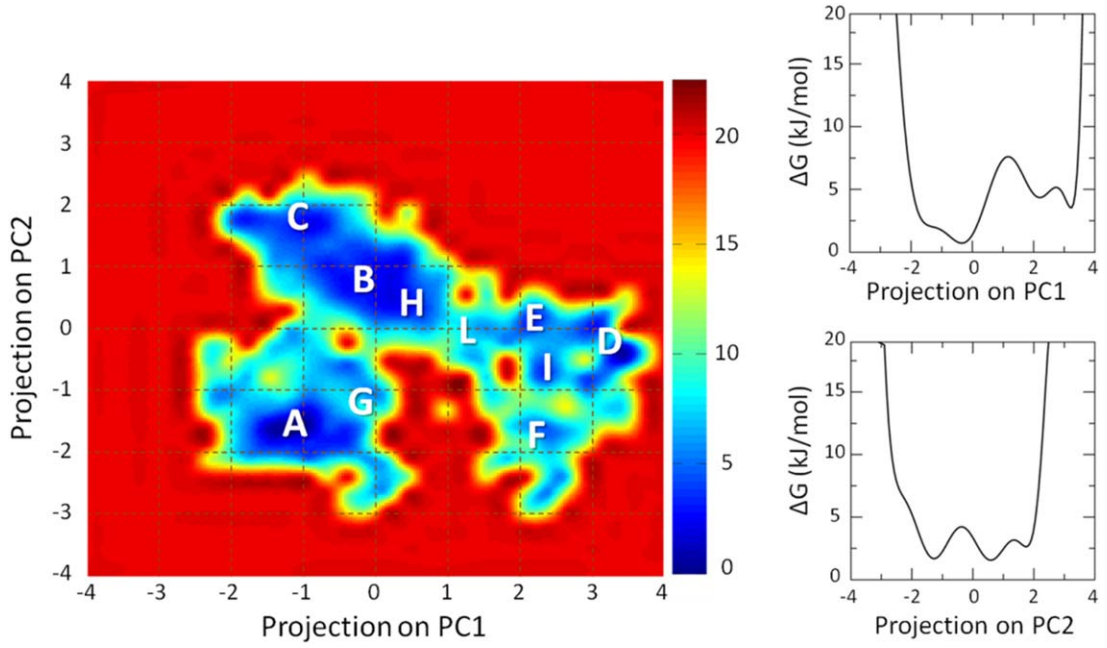

Figure 5

On the left the free-energy profile (kJ/mol) of the AXH^m are represented as function of the first and second principal component projection. Labels indicate the position on the free-energy landscape (in term of first and second principal component projection values) of cluster centroids obtained by structure based clustering approach on the REMD trajectory at 310 K. The 1D free energy profiles as function of each principal component projection are reported on the right panels.

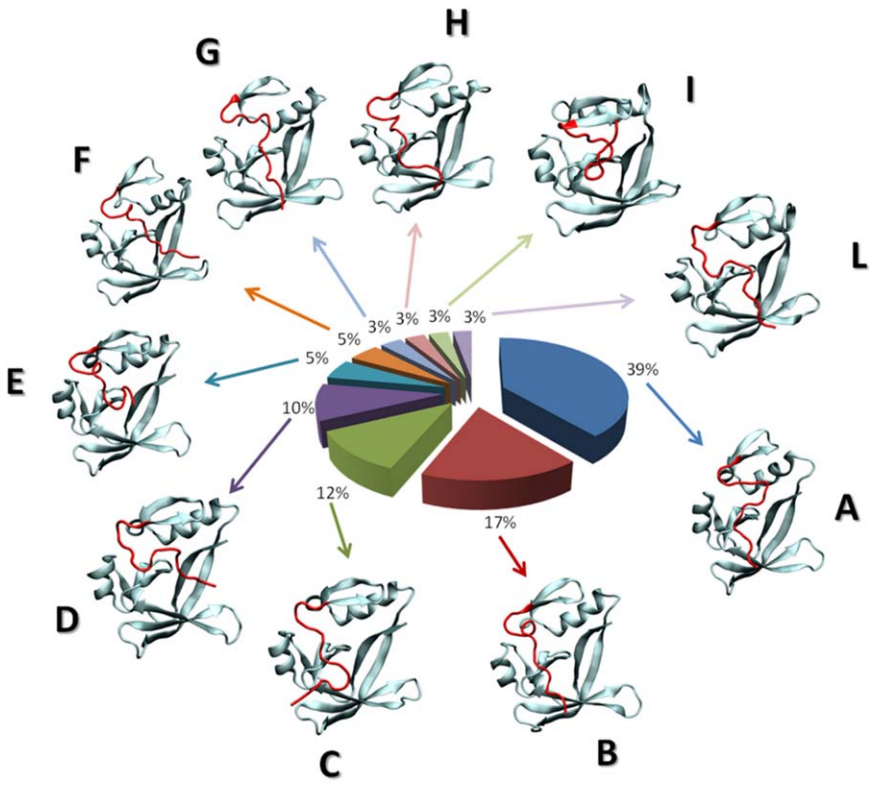

Figure 6

Structure based clustering analysis on REMD trajectory at 310 K. Cluster centroids are also shown and labeled. Clusters not shown are characterized by a percentage population lower than 2% over the whole trajectory steps. [Color figure can be viewed in the online issue, which is available at wileyonlinelibrary.com.]

The free energy barrier that separate the previously mentioned minima lie in range 5–10 kJ/mol demonstrating that the AXH^m may overcome the energy barriers under the thermal fluctuation, moving from one state to another. These findings suggest that, despite the well-defined and conserved secondary structure (Fig. 2), the AXH^m alone in water environment is characterized by extensive conformational fluctuation of the N-terminal region, as previously reported for classical MD simulation.

In view of already known AXH crystal structure,[1,9] it is interesting to highlight how the experimentally solved conformations fall in the estimated free-energy landscape (Supporting Information Figs. S3–S5).

The three available Protein Data Bank (PDB) models containing AXH tetramers (1OA8, 4APT, and 4AQP) have been represented in terms of first and second principal component projection values for each monomer, called a, b, c, and d (Supporting Information Figs. S3–S5). In all cases, PDB models fall in free energy areas close to those covered by clusters B and H, suggesting that our results in term of free energy landscape are consistent with experimental observations. Of interest is the finding that none of the PDB models fall into energy wells close to cluster A (the most populated REMD cluster) indicating that this specific N-ter arrangement is not achieved in a dimeric or tetrameric form.

DISCUSSION

Ataxin-1 is an RNA-binding protein responsible for the spinocerebellar ataxia type 1, a neurodegenerative disease associated with protein misfolding and aggregation. Despite the well-established relationship between polyglutamine tract expansion and disease onset and severity, the AXH domain of Ataxin 1 is involved in the protein aggregation mechanism, modulating the aggregation of the full-length protein.[5] The isolated AXH domain spontaneously misfolds and forms amyloid fibers *in vitro* without the presence of any destabilizing conditions.[5] Moreover, the replacement of the AXH domain with the homologous sequence from the transcription factor HBP1, which has no tendency to spontaneously aggregate, has determined the reduction of Ataxin-1 aggregation. On the other hand, the AXH domain plays also a key role in the physiological function of Ataxin-1, because of its transcriptional repression activity and of its role in a huge number of intermolecular interactions

with different cellular partners[9] including SMRT/SMRTER and Capicua proteins.[11] The crystal structure of the isolated AXH domain contains two globular dimers (i.e., four AXH molecules), with the protomers characterized by asymmetric dimer interfaces. Despite the sharing of the secondary structure, the N-terminal region of the AXH domain is characterized by a conformational heterogeneity already described by experimental works.[7] These findings have raised the interesting issue of whether the conformational flexibility is (i) an intrinsic feature of the AXH monomer, (ii) an artifact of crystallization or, (iii) dependent on the monomer–monomer interaction.[9] A recent experimental study has demonstrated that the AXH aggregation and misfolding are impaired by the interaction between AXH^m and its cellular partner, i.e. the transcriptional regulator CIC peptide.[13] This finding has led to suggest a strategy for preventing AXH aggregation by using CIC peptide as a template to design peptide-mimetic molecules able to stabilize the AXH^m.[13] In detail, the AXH physiological interactions are able to shift the equilibrium between monomeric and dimeric species toward the monomer. A leading role in these physiological interactions is played by the AXH domain N-terminus; that is, drastically stabilized.

In this connection, here we have provided the first computational description of the AXH^m conformational fluctuations through a characterization at atomistic level of the AXH monomer in water by means of both biased and unbiased MD simulations. We have applied an approach that combines the extraction of collective motions with the sampling of its free energy surface, as was successfully previously done in literature.[36,39] This method brings together the efficient sampling of REMD with a dimensionality reduction technique. In particular, PCA was used to elucidate the collective motion maximally related to the conformational fluctuation of the N-terminal region of the AXH^m, and the REMD simulation was carried out to deeply sample the state space and to calculate the corresponding free-energy landscape.

Recently, it has been suggested that the AXH^m might be unstable because its sickle-cell shape leaves the protein hydrophobic core exposed.[9] Here, we have shown that the AXH^m in water environment is generally stable for temperature ranging from 310 to 450 K, with the exception of the N-terminal region (Figs. 1 and 5). In fact, one of the most important result of the present work is that, although the AXH^m is characterized by a well-preserved secondary structure (Fig. 2), the N-terminal region has shown an intrinsic tendency to accomplish a wide range of conformational changes (Figs. 1 and 5). These structural fluctuations are well described analyzing the MD trajectory along the first two Principal Components (Figs. 3 and 4), used in this work to estimate the corresponding free energy landscape. The identified free energy wells (Fig. 5) are separated by an energy barrier of about 5–10 kJ/mol demonstrating that the AXH^m may overcome this barriers under the thermal fluctuation, moving from one low-energy state to another. These findings suggest that, despite the well-defined and conserved secondary structure (Fig. 2), the AXH^m alone in water environment is characterized by extensive conformational fluctuations of the N-terminal region (clusters A to H, Figs. 5 and 6). Moreover, our results have highlighted that available PDB models fall only in free energy areas corresponding to clusters B and H (Supporting Information Figs. S3–S5). Therefore the specific N-ter arrangement characterizing cluster A (the most likely for the AXH^m) has never been observed in a dimeric or tetrameric form.[1,9] It is plausible that the interactions leading to the dimer formation might be able to stabilize the N-ter region of the AXH^m, which is involved in the dimeric interface or, viceversa, that this arrangement favors the dimerization by affecting the kinetics.

Starting from the assumption that the equilibrium of the monomer/dimer/tetramer species of the AXH represents an important point of the aggregation pathway of the Ataxin-1,[40] further work is needed to better clarify the importance of the monomer–monomer interaction in the structural and dynamics properties of the AXH domain. In agreement with previous experimental findings,[13] our results can be considered as a basis for a future design of ataxin aggregation inhibitors that will require several key conformations identified in the present study as molecular targets for ligand binding.

CONCLUSIONS

Our work points out the attention on N-terminal fluctuations of Ataxin 1 providing evidences on several possible conformations which may be accessible in the AXH monomeric form. Those monomeric conformations fall into energy minima separated by low energy barriers, indicating that the AHX^m N-terminal arrangement can switch continuously from a configuration to another under the effect of thermal fluctuations. Nevertheless, experimental data on AHX dimers and tetramers suggest that few of the above shown N-ter conformational states are actually accessible in aggregated AHX. Therefore, a relationship may possibly exist between AXH dimerization kinetics and N-ter flexibility. In this sense, our work provides a number of AXH models for further investigations on AXH dimers to shed light on molecular mechanism behind AXH aggregation. Moreover, on the basis of insights coming from these further studies, novel aggregation inhibitors might be designed to drive N-ter conformational changes in order to reduce the monomer–monomer binding affinity and destabilize dimeric and tetrameric aberrant aggregates.

REFERENCES

1. Chen YW, Allen MD, Veprintsev DB, Löwe J, Bycroft M. The structure of the AXH domain of Spinocerebellar Ataxin-1. J Biol Chem 2004;279:3758–3765.
2. Zoghbi HY, Orr HT. Pathogenic mechanisms of a polyglutamine-mediated neurodegenerative disease, Spinocerebellar ataxia type 1. J Biol Chem 2009;7425–7429.
3. Emamian ES, Kaytor MD, Duvick LA, Zu T, Tousey SK, Zoghbi HY, Clark HB, Orr HT. Serine 776 of ataxin-1 is critical for polyglutamine-induced disease in SCA1 transgenic mice. Neuron 2003;38:375–387.
4. Klement IA, Skinner PJ, Kaytor MD, Yi H, Hersch SM, Clark HB, Zoghbi HY, Orr HT. Ataxin-1 nuclear localization and aggregation: role in polyglutarnine-induced disease in SCA1 transgenic mice. Cell 1998;95:41–53.
5. De Chiara C, Menon RP, Dal Piaz F, Calder L, Pastore A. Polyglutamine is not all: the functional role of the AXH domain in the ataxin-1 protein. J Mol Biol 2005;354:883–893.
6. Saunders HM, Bottomley SP. Multi-domain misfolding: understanding the aggregation pathway of polyglutamine proteins. Protein Eng. Des. Sel. 2009:447–451.
7. De Chiara C, Menon RP, Adinolfi S, de Boer J, Ktistaki E, Kelly G, Calder L, Kioussis D, Pastore A. The AXH domain adopts alternative folds the solution structure of HBP1 AXH. Structure 2005;13: 743–53.
8. De Chiara C, Giannini C, Adinolfi S, de Boer J, Guida S, Ramos A, Jodice C, Kioussis D, Pastore A. The AXH module: an independently folded domain common to ataxin-1 and HBP1. FEBS Lett 2003;551:107–112.
9. De Chiara C, Rees M, Menon RP, Pauwels K, Lawrence C, Konarev PV, Svergun DI, Martin SR, Chen YW, Pastore A. Self-assembly and conformational heterogeneity of the AXH domain of ataxin-1: an unusual example of a chameleon fold. Biophys J 2013;104:1304–1313.
10. Tsuda H, Jafar-Nejad H, Patel AJ, Sun Y, Chen HK, Rose MF, Venken KJT, Botas J, Orr HT. The AXH domain of ataxin-1 mediates neurodegeneration through its interaction with Gfi-1/senseless proteins. Cell 2005;122:633–644.
11. De Chiara C, Pastore A. Polyglutamine diseases and neurodegeneration: the example of ataxin-1. Supramolecular structure and function 10. Dordrecht: Springer; 2011. pp 87–99.
12. Menon RP, Soong D, de Chiara C, Holt M, McCormick JE, Anilkumar N, Pastore A. Mapping the self-association domains of ataxin-1: identification of novel non overlapping motifs. Peer J 2014;2:e323.
13. De Chiara C, Menon RP, Kelly G, Pastore A. Protein–protein interactions as a strategy towards protein-specific drug design: the example of ataxin-1. In: Cavalli A, editor. PLoS One 2013;8:e76456.
14. Deriu MA, Soncini M, Bidone T, Redaelli A, Montevecchi FM. Coarse grain modeling for microtubule mechanics. Mater Sci Forum Trans Tech Publ 2010;6:629–634.
15. Paciello G, Acquaviva A, Ficarra E, Deriu MA, Macii E. A molecular dynamics study of a miRNA:mRNA interaction. J Mol Model 2011; 17:2895–2906.
16. Bidone TC, Kim T, Deriu MA, Morbiducci U, Kamm RD. Multiscale impact of nucleotides and cations on the conformational equilibrium, elasticity and rheology of actin filaments and crosslinked networks. Biomech Model Mechanobiol 2015.
17. Gentile F, Deriu M, Licandro G, Prunotto A, Danani A, Tuszynski J. Structure based modeling of small molecules binding to the TLR7 by atomistic level simulations. Molecules 2015;20:8316–8340.
18. Deriu MA, Bidone TC, Mastrangelo F, Di Benedetto G, Soncini M, Montevecchi FM, Morbiducci U. Biomechanics of actin filaments: a computational multi-level study. J Biomech 2011;44:630–636.
19. Shema-Mizrachi M, Pavan GM, Levin E, Danani A, Lemcoff NG. Catalytic chameleon dendrimers. J Am Chem Soc 2011;133:14359–14367.
20. Deriu MA, Grasso G, Licandro G, Danani A, Gallo D, Tuszynski JA, Morbiducci U. Investigation of the Josephin domain protein–protein interaction by molecular dynamics. In: Salahub D, editor. PLoS One 2014;9:e108677.
21. Grasso G, Deriu MA, Prat M, Rimondini L, Vernè E, Follenzi A, Danani A. Cell penetrating peptide adsorption on magnetite and silica surfaces: a computational investigation. J Phys Chem B 2015; 119:150604120603009.
22. Apicella A, Soncini M, Deriu MA, Natalello A, Bonanomi M, Dellasega D, Tortora P, Regonesi ME, Casari CS. A hydrophobic gold surface triggers misfolding and aggregation of the amyloidogenic Josephin domain in monomeric form, while leaving the oligomers unaffected. PLoS One 2013;8:e58794.
23. Berendsen HJC, Postma JPM, Van Gunsteren WF, DiNola A, Haak JR. Molecular dynamics with coupling to an external bath. J Chem Phys 1984;81:3684–3690.
24. Hess B, Kutzner C, van der Spoel D, Lindahl E. GROMACS 4: algorithms for highly efficient, load-balanced, and scalable molecular simulation. J Chem Theory Comput 2008;4:435–447.
25. Hornak V, Abel R, Okur A, Strockbine B, Roitberg A, Simmerling C. Comparison of multiple Amber force fields and development of improved protein backbone parameters. Proteins 2006;65:712–725.
26. Lindorff-Larsen K, Piana S, Palmo K, Maragakis P, Klepeis JL, Dror RO, Shaw DE. Improved side-chain torsion potentials for the Amber ff99SB protein force field. Proteins 2010;78:1950–1958.
27. Lindorff-Larsen K, Maragakis P, Piana S, Eastwood MP, Dror RO, Shaw DE. Systematic validation of protein force fields against experimental data. PLoS One 2012;7:e32131.
28. Jorgensen WL, Chandrasekhar J, Madura JD, Impey RW, Klein ML. Comparison of simple potential functions for simulating liquid water. J Chem Phys 1983;79:926.
29. Hess B, Bekker H, Herman JC, Berendsen J, Fraaije GEM. LINCS: a linear constraint solver for molecular simulations. J Comput Chem 1997;18:1463–1472.
30. Bussi G, Donadio D, Parrinello M. Canonical sampling through velocity rescaling. J Chem Phys AIP;2007;126:014101.
31. Humphrey W, Dalke A, Schulten K. VMD: visual molecular dynamics. J Mol Graph 1996;14:33–38.
32. Frishman D, Argos P. Knowledge-based protein secondary structure assignment. Proteins 1995;23:566–579.
33. Heinig M, Frishman D. STRIDE: a web server for secondary structure assignment from known atomic coordinates of proteins. Nucleic Acids Res 2004;32:W500–W502.
34. Laskowski RA, MacArthur MW, Moss DS, Thornton JM. PROCHECK: a program to check the stereochemical quality of protein structures. J Appl Crystallogr 1993;26:283–291.
35. Sugita Y, Okamoto Y. Replica-exchange molecular dynamics method for protein folding. 1999;141–151.
36. Nguyen PH, Stock G, Mittag E, Hu CK, Li MS. Free energy landscape and folding mechanism of a β-hairpin in explicit water: a replica exchange molecular dynamics study. Proteins Struct Funct Genet 2005;61:795–808.
37. Daura X, Gademann K, Jaun B, Seebach D, van Gunsteren WF, Mark AE. Peptide folding: when simulation meets experiment. Angew Chem Int Ed 1999;38:236–240.
38. Maisuradze GG, Liwo A, Scheraga H. A principal component analysis for protein folding dynamics. J Mol Biol 2009;385:312–329.
39. Lazim R, Mei Y, Zhang D. Replica exchange molecular dynamics simulation of structure variation from α/4β-fold to 3α-fold protein. J Mol Model 2012;18:1087–1095.
40. De Chiara C, Pastore A. Kaleidoscopic protein–protein interactions in the life and death of ataxin-1: new strategies against protein aggregation. Trends Neurosci 2014;37:211–218.